Inorganic Chemistry

ARTICLE

pubs.acs.org/IC

Modification in Structure, Phase Transition, and Magnetic Property of Metallic Gallium Driven by Atom−Molecule Interactions

Le Xin Song,* Jie Chen, Lin Hong Zhu, Juan Xia, and Jun Yang

Department of Chemistry, University of Science and Technology of China, Hefei 230026, P. R. China

Supporting Information

ABSTRACT: The present work supports a novel paradigm in which the surface structure and stacking behavior of metallic gallium (Ga) were significantly influenced by the preparation process in the presence of organic small molecules (ethanol, acetone, dichloromethane, and diethyl ether). The extent of the effect strongly depends on the polarity of the molecules. Especially, a series of new atom−molecule aggregates consisting of metallic Ga and macrocyclic hosts (cyclodextrins, CDs) were prepared and characterized by various techniques. A comprehensive comparative analysis between free metallic Ga and the Ga samples obtained provides important and at present rare information on the modification in structure, phase transition, and magnetic property of Ga driven by atom−molecule interactions. First, there is a notable difference in microstructure and electronic structure between the different types of Ga samples. Second, differential scanning calorimetry analysis gives us a complete picture (such as the occurrence of a series of metastable phases of Ga in the presence of CDs) that has allowed us to consider that Ga atoms were protected by the shielding effect provided by the cavities of CDs. Third, the metallic Ga distributed in the aggregates exhibits very interesting magnetic property compared to free metallic Ga, such as the uniform zero-field-cooled and field-cooled magnetization processes, the enhanced responses in magnetization to temperature and applied field, and the fundamental change in shape of magnetic hysteresis loops. These significant changes in structural transformation and physical property of Ga provide a novel insight into the understanding of atom−molecule interactions between metallic atoms and organic molecules.

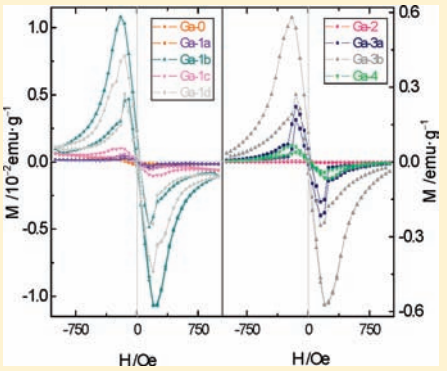

INTRODUCTION

Metallic gallium (Ga) is one of metals that have extraordinarily low melting points and has great significance in the production of semiconductors.[1−3] Because of its special physical and chemical properties, there have been numerous reports on the results of atomic and electronic structures and complicated phases.[4−6] Also, Ga is able to form alloys with many metals and especially Ga-doped hybrid materials, showing great promise for use in the fabrication of optoelectronic and microelectronic devices.[7−10] Cyclodextrins (CDs, macrocyclic hosts) are a group of cyclic oligosaccharides composed of α-1,4-linked glucose units, capable of forming inclusion complexes with many guests owing to their hydrophobic cavity surrounded by a hydrophilic outer surface.[11−15] There are numerous reports about the effect of CDs on physical aspects of guests, such as organic molecules, inorganic ions, and coordination compounds.[16−19] This effect was attributed to intermolecular interaction and molecule−ion interaction between host and guest.[20,21] Nevertheless, there have been rare reports of possible interactions between metal atoms and host molecules.[22]

All of these considerations impel us to examine whether there is an atom−molecule interaction between metal atoms and organic molecules. If yes, this will lead to the following two questions. 1) How does the presence of organic solvent media with low boiling points affect the crystallization of Ga? And 2) how does the doping of small amounts of organic hosts impact the structure, phase transition, and magnetic property of Ga? In the present work, we try to address these issues.

Initially, four types of metallic Ga samples crystallized in the presence of solvents: ethanol (Ga−1a), acetone (Ga−1b), dichloromethane (Ga−1c), and diethyl ether (Ga−1d) were prepared and characterized by X-ray diffraction (XRD) and field-emission scanning electron microscopy (FE-SEM). All of the Ga samples are still pure because no solvents were found to remain in the Ga phases. However, their microstructures are distinct from each other and from unprocessed Ga phase. Further, a close relationship between the crystallization of Ga and the polarity of the solvents was found, that is, the lower polarity the solvents used, the larger the size of the Ga crystals obtained, the looser the structure.

Next, seven forms of metallic Ga samples doped by adding macrocyclic host molecules like α- (Ga−2), β- (Ga−3 series samples) and heptakis(2,6-di-*O*-methyl)-β-CD (DMβ-, Ga−4) using acetone as a solvent medium were obtained and measured by XRD, FE-SEM, X-ray photoelectron spectroscopy (XPS), differential scanning calorimetry (DSC), and a superconducting quantum interference device (SQUID). Our results indicate that the addition of CDs results in a significant change in surface structure, atom arrangement, and electronic property of metallic

Received: January 20, 2011
Published: August 02, 2011

Ga. Such a change is ascribed to the influence of atom−molecule interactions between Ga atoms and CD molecules. Different interactions were found to produce different effects on the transition behavior of multiphases of Ga. In addition, SQUID measurements provide important information on the modification of magnetic property of Ga in the presence of CD molecules.

In short, the present study provides the first example of discussing atom−molecule interactions between a metal atom and a series of organic molecules and consequential effects. We believe this work will be particularly important to understanding the modification in structure and physical properties of metallic crystals.

EXPERIMENTAL SECTION

Materials. α- and β-CD were purchased from Nihon Toshin Chemical Company and Shanghai Chemical Reagent Company, respectively. DMβ-CD was kindly donated by Harata. Metallic Ga, anhydrous ethanol, and diethyl ether were obtained from Sinopharm Chemical Reagent Company. Acetone and dichloromethane were supplied by Yangzhou Hubao Chemical Reagent Company and Jiangsu Qiangsheng Chemical Reagent Company respectively and dried with anhydrous sodium sulfate before use. All other chemicals were of general-purpose reagent grade unless otherwise stated and kept under the same conditions.

Preparation of Ga Samples. The low melting point of Ga makes it easily dispersed as liquid state at a low temperature. Several Ga samples were prepared according to the following procedure and marked as follows. Metallic Ga (500 mg, 7.17 mmol) was added to 10 mL anhydrous ethanol in a round-bottom flask with a ground glass cap, followed by vigorous stirring at 320.2 K for 5 h. The liquid sample was then in the bottle with sealing tape perforated with several small holes. The solvent was allowed to slowly and completely evaporate at room temperature. A few weeks later, the Ga sample was obtained and marked as Ga−1a. The other three Ga samples, Ga−1b, Ga−1c, and Ga−1d were prepared in the same manner but using acetone, dichloromethane, and diethyl ether as a solvent medium, respectively. All of the Ga samples were obtained and measured under the same drying conditions. The densities from Ga−1a to Ga−1d were determined to be 5.38, 5.38, 5.21, and 5.04 $g \cdot cm^{-3}$, respectively.

Furthermore, metallic Ga (500 mg, 7.17 mmol) was added to 10 mL acetone in the presence of α-CD (50 mg, 5.14×10^{-2} mmol) in a round-bottom flask with vigorous stirring at 320.2 K for 5 h. After the solvent was evaporated in air at room temperature, the Ga sample containing α-CD was obtained and marked as Ga−2. Ga−3a and Ga−4 were obtained in the same method (a 10:1 mass ratio of Ga to a CD) but using β-, and DMβ-CD, respectively.

Finally, the Ga sample consisting of metallic Ga (500 mg, 7.17 mmol) and β-CD (5 mg, 4.40×10^{-3} mmol) in a 100:1 mass ratio using 10 mL acetone as a solvent medium at 320.2 K for 5 h was obtained and labeled as Ga−3b. Other three Ga samples: Ga−3c, Ga−3d, and Ga−3e were obtained in the same method with mass ratios of 250:1, 500:1, and 1000:1 respectively to investigate the effect of the Ga/β-CD ratios on the Ga properties. The control sample of Ga without treatment was marked as Ga−0.

Sintering Experiments. Samples containing β-CD (1135 mg, 1 mmol) using 10 mL acetone as a solvent medium in the absence and presence of metallic Ga (69.7 mg, 1 mmol) were prepared at 320.2 K for 5 h and dried to constant weight before sintering. Calcinations of the two samples were conducted in a tube furnace (Nabertherm, M7/11, with a program controller) at 773.2 K for 0.5 h in nitrogen atmosphere. Then they were cooled down to room temperature in a desiccator over P_2O_5 after sintering and weighted. The Ga sample obtained from the sintering experiment was labeled as Ga−3f.

Instruments and Methods. All solid samples were kept and measured under the same drying conditions. XRD measurements were carried out on a Philips X'Pert Pro X-ray diffractometer using a monochromatized Cu Kα radiation source (40 kV, 40 mA) with a wavelength of 0.1542 nm and analyzed in the range $5° \le 2\theta \le 85°$. Photographs of the Ga−1 series samples were taken with a camera after the solvents were evaporated. FE-SEM images were obtained from the samples dispersed in acetone on a Supra 40 FE-SEM operated at 5 kV.

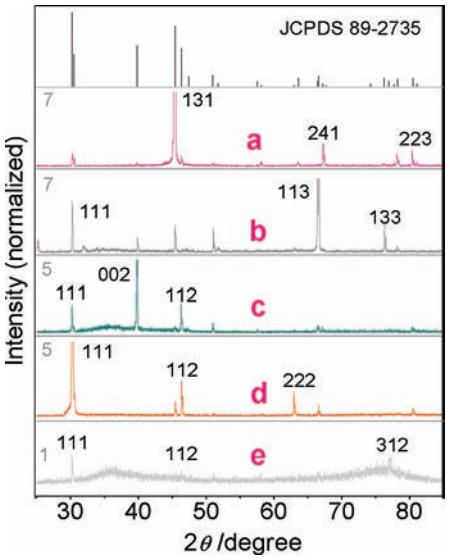

Figure 1. XRD patterns of (a) Ga−0, (b) Ga−1a, (c) Ga−1b, (d) Ga−1c, and (e) Ga−1d. Relative signal intensity was normalized to the intensity of the peak at 30.2° in curve e.

Elemental analysis was performed on an Elementar Vario EL III elemental analyzer. The gallium content in samples was determined by flame atomic absorption spectrometry (FAAS) using a PerkinElmer AAnalyst 800 (PerkinElmer, USA). The result of elemental analysis: Ga−2, Anal. Calcd for $Ga \cdot 0.0064(C_{36}H_{60}O_{30} \cdot 6H_2O)$: Ga, 90.91; C, 3.63; H, 0.61. Found: Ga, 90.69; C, 3.71; H, 0.65. Ga−3a, Anal. Calcd for $Ga \cdot 0.0055(C_{42}H_{70}O_{35} \cdot 7H_2O)$: Ga, 90.91; C, 3.63; H, 0.61. Found: Ga, 91.16; C, 3.47; H, 0.54. Ga−3b, Anal. Calcd for $Ga \cdot 0.00055$ $(C_{42}H_{70}O_{35} \cdot 7H_2O)$: Ga, 99.01; C, 0.40; H, 0.07. Found: Ga, 98.80; C, 0.47; H, 0.10. Ga−4, Anal. Calcd for $Ga \cdot 0.0048(C_{56}H_{98}O_{35} \cdot 7H_2O)$: Ga, 90.91; C, 4.20; H, 0.71. Found: Ga, 91.09; C, 4.04; H, 0.63. No carbon and hydrogen were detected in the Ga−1 series samples. XPS measurement was done using an ESCALAB250 spectrometer, with Al Kα excitation radiation (1486.6 eV) in ultrahigh vacuum conditions (2.00×10^{-9} Torr). And all of the values of binding energy were referenced to C1s peak (284.6 eV) with an energy resolution of 0.16 eV.

Thermogravimetry (TG) and derivative thermogravimetry (DTG) analyses were made on a DTGA-60H thermogravimetric analyzer at a constant heating rate of 10.0 $K \cdot min^{-1}$ under a nitrogen atmosphere with a gas flow of 25 $mL \cdot min^{-1}$. Raman spectra were recorded with a LABRAM-HR Confocal Laser MicroRaman spectrometer at room temperature with 514.5 nm laser excitation in the range 800−3500 cm^{-1}, with a resolution of 0.6 cm^{-1}. DSC measurements were conducted on a DSCQ2000 at a constant heating and cooling rate of 10.0 $K \cdot min^{-1}$ for three cycles under a nitrogen atmosphere with a gas flow of 50 $mL \cdot min^{-1}$.

Magnetic measurements of the samples, including temperature and field dependences of magnetization, were obtained with a Quantum Design (QD, San Diego, USA) Magnetic Properties Measurement System (MPMS-7XL) equipped with a SQUID by means of a vibrating sample magnetometer (VSM).

RESULTS AND DISCUSSION

Effects of Organic Solvent Media on the Crystallinity of Ga. Four organic solvents: ethanol, acetone, dichloromethane,

dx.doi.org/10.1021/ic200137f |Inorg. Chem. 2011, 50, 7988–7996

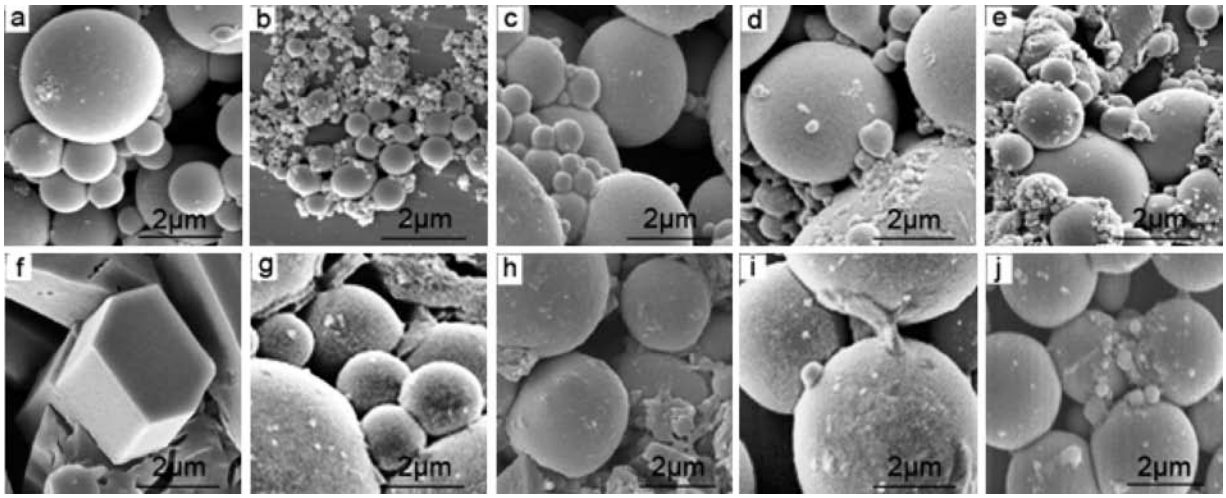

Figure 2. FE-SEM images of (a) Ga−0, (b) Ga−1a, (c) Ga−1b, (d) Ga−1c, (e) Ga−1d, (f) β-CD, (g) Ga−2, (h) Ga−3a, (i) Ga−3b, and (j) Ga−4.

and diethyl ether were used to examine whether changes in solvent polarities during dispersion were related to the crystallization of Ga and, if yes, to what degree. Figure 1 illustrates the XRD patterns of Ga−0 and the crystallized Ga samples (Ga−1a∼d).

As seen in part a of Figure 1, the diffraction signals of the free metallic Ga match best to an end-centered orthorhombic structure with cell parameters: a = 0.4523 nm, b = 0.7661 nm, c = 0.4524 nm (JCPDS # 89−2735). However, upon dispersion, the metallic Ga samples are in good agreement with an end-centered orthorhombic structure in JCPDS # 89−2735,[23] and exhibit completely different stacking sequences, each having a characteristic close packed plane (CCPP). For example, the CCPP values of Ga−1a, Ga−1b and Ga−1c are 113 (66.6°), 002 (39.9°), and 111 (30.3°), respectively. The shift of diffraction peaks corresponding to the CCPP values toward lower 2θ angles from Ga−1a, Ga−1b to Ga−1c, Ga−1d reveals that dispersion effects of the organic solvents are dependent on the nature of solvent media used.

Interestingly, the increase in the distance (d) between the CCPP values in the order: Ga−1a (0.141 nm) < Ga−1b (0.226 nm) < Ga−1c (0.295 nm) is in good accord with the decrease order of polarity of the solvents: ethanol > acetone > dichloromethane. Nevertheless, the XRD pattern of Ga−1d indicates a poor crystallinity, and no CCPP signal was detected, which is probably related to the low polarity of diethyl ether.

Photographs indicate that Ga−0 shows a large blocky morphology, but the four Ga−1 series samples exhibit smaller crystal size, in particular those derived from ethanol and acetone.[24] The changes in size and appearance reveal that the lower polarity the solvents used, the larger the size of the Ga crystals obtained, and the looser the structure based on density evolution.

Parts a−e of Figure 2 present FE-SEM images of free Ga and the Ga−1 series samples. The particles of all the metallic Ga samples are declared to have a sphere-like shape, and diameter between 0.2 and 2.5 μm. Apparently, the effect of solvent media on the surface structure of metallic Ga is reflected by the difference in diameter rather than in shape. For example, Ga−1a exhibits the smallest average size (200 to 500 nm), showing the effect of organic solvents.

These phenomena provide direct evidence for the effect of organic solvents on the crystallinity of Ga. It allows us to consider that the crystal growth of Ga was regulated by van der Waals interactions between organic molecules and Ga atoms. Undoubtedly, different dispersion systems were involved in different intensities of van der Waals interactions. Liquid Ga is metallic, whereas in the solid state two Ga atoms form covalently bound Ga_2 molecules with weak intermolecular interactions.[6] During the dispersion process between two fluids (liquid Ga and solvents), different intensities of van der Waals interactions result in different stacking forms of Ga crystals. The effect of organic solvents on the crystallinity of Ga leads us to consider the possibility of inclusion complexation between an organic host molecule and Ga atoms.

Microstructure and Electronic Structure of Ga in the Presence of CDs. First, β-CD was used as the host because it is a cyclic oligosaccharide with a hydrophobic cavity in the molecule center, and acetone with a moderate polarity was used as the solvent medium to produce a homogeneous effect.

FE-SEM images in parts f and c of Figure 2 show that the crystal morphologies of free β-CD and Ga−1b are formed in a right regular hexagonal prism with nearly square prism faces and a sphere of different particle diameters from 250 nm to 2.5 μm, respectively. Nevertheless, the surface structure of Ga−3a in part h of Figure 2 gives completely different features: both the occurrence of a large number of small spheres of similar diameters (2−3 μm) and the presence of anomalous fragments. Clearly, the presence of β-CD improves the crystallization of Ga conditions to such a level that more stable bulk Ga crystals are predominantly formed in a uniform sphere. This is attributable to an interaction between β-CD molecules and Ga atoms. Also, the interaction has caused β-CD crystals and small spheres of Ga to become cracked or broken.

Second, such a significant transformation in the surface structure and crystal orientation of Ga also occurs in the cases of α-CD and DMβ-CD. Parts g and j of Figure 2 indicate the FE-SEM images of Ga in the presence of the two CDs. Apparently, the presence of α-CD causes the size of all the Ga particles to become larger relative to the unaffected ones (part g of Figure 2). DMβ-CD appears to have a highly similar effect as the parent β-CD on the formation of Ga microcrystals.

These cases provide an important clue to the cause of the effect of CDs. The fact that the effect of modification of 14 hydroxyl groups of β-CD differs from the effect of cavity diameter gives an

dx.doi.org/10.1021/ic200137f |*Inorg. Chem.* 2011, 50, 7988–7996

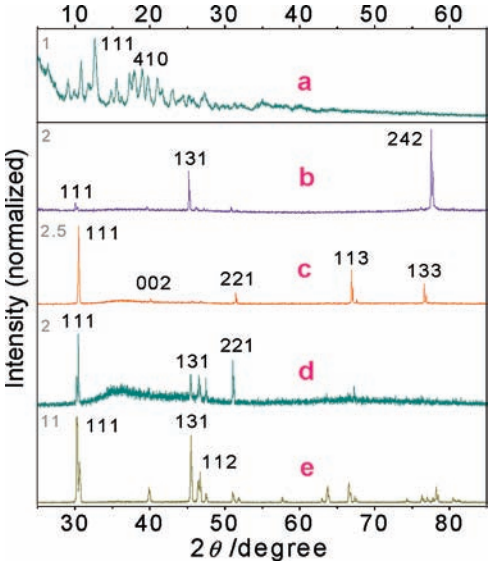

Figure 3. XRD patterns of (a) β-CD, (b) Ga−2, (c) Ga−3a, (d) Ga−3b, and (e) Ga−4. Relative signal intensity was normalized to the intensity of the peak at 12.6° in curve a.

impression that the hydrophobic cavity in CDs may play a role in modulating the size and shape of the particles via an intercalation interaction between Ga atoms and CD cavities. The diameter comparison between Ga atoms (0.36 nm) and cavities of CDs (α-, 0.47−0.53 nm; β- and DMβ-CD, 0.60−0.65 nm) shows that this intercalation interaction is more efficient for the β- or DMβ-CD. Hence, the interaction in this case makes a significant contribution to the growth of Ga particles through prohibiting the excessive aggregation of Ga particles. This observation is supported by the finding that the lower the initial molar ratio of β-CD to Ga, the larger size the Ga particles obtained (part I of Figure 2).

Parts a and c of Figure 3 depict the XRD patterns of β-CD and Ga−3a. Three main diffraction peaks of free β-CD occur at 9.1 (101), 12.6 (111), and 19.0° (410). However, they are not observable in the XRD pattern of Ga−3a. And the very intense diffraction peak at about 39.9° (002) in the XRD pattern of Ga−1b (part c of Figure 1) is seriously weakened in the case of Ga−3a.

The XRD result in part c of Figure 3 suggests that the crystallographic phase of the Ga particles in Ga−3a belongs to an end-centered orthorhombic lattice (JCPDS # 89−2735). The sample exhibits a rather different crystal structure from either free β-CD or Ga−1b. For example, no peaks due to β-CD are found at low angles as a consequence of the breakdown of its stacking structure, which is in good accordance with the SEM analysis above. Also, there is a CCPP (111) at 30.6° (d, 0.292 nm) in the crystal with a high degree of order as evidenced by the presence of the sharp peaks in the XRD photograph. A probable recombination in the Ga−3a that generated a structural change is supported by the change of CCPP and the distinct shift ($\Delta 2\theta$, 0.4°) of the diffraction peak corresponding to the 111 plane from 30.2° (Ga−1b) to 30.6° (Ga−3a).

The XRD patterns of the three samples (Ga−2, Ga−3b, and Ga−4) in Figure 3 show that there is a considerable difference in the crystallization of Ga between the samples and Ga−3a. Obviously, all the three Ga samples (Ga−3a, Ga−3b, and Ga−4) obtained from the systems of β-CD and its derivative

Table 1. Binding Energies (eV) of Some Core Levels in the Samples

	Binding energy (eV)				
samples	Ga 3d	Ga $2p_{3/2}$	Ga $2p_{1/2}$	C 1s	O 1s
β-CD				284.6, 286.3, 287.7	532.8
Ga−0	18.7	1116.7	1143.5		
Ga−1b	18.0	1118.0	1143.6		
Ga−3a	18.2	1118.7	1144.7	282.0	530.0

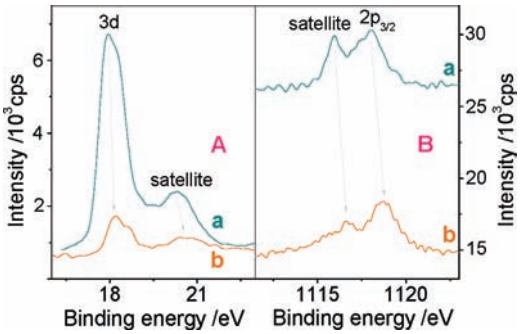

Figure 4. Ga 3d (A) and Ga $2p_{3/2}$ (B) XPS spectra of (a) Ga−1b and (b) Ga−3a.

show the strongest peak at a similar position (30.4−30.6°), corresponding to the same CCPP (111). However, the strongest peak of the Ga sample (Ga−2) obtained from the system of α-CD appears at a much higher 2θ angle (77.5°), corresponding to a CCPP (242). The result supports the view that the cavity diameter of CDs exerts a more dominant effect in regulating the crystal growth of metallic Ga.

The surprising results from these observations (FE-SEM and XRD) strongly imply the existence of an atom−molecule interaction between Ga atoms and CDs and further prompt us to hypothesize a relationship between the atom−molecule interaction and the electronic structure of Ga.

XPS experiments were performed to probe some specific aspects of Ga deposition processes.[25] Table 1 summarized the binding energies of Ga 3d, Ga $2p_{3/2}$, and Ga $2p_{1/2}$ in the Ga samples (Ga−0, Ga−1b, and Ga−3a) as well as those of C 1s and O 1s in the β-CD samples (β-CD[26] and Ga−3a).

Analysis of the data provides two important insights. First, the Ga sample (Ga−1b) processed by acetone has a lower binding energy of Ga 3d but higher binding energies of Ga $2p_{3/2}$ and Ga $2p_{1/2}$ compared to the free Ga sample. The increase in electron density of the 3d inner-shell region and the decrease in electron density of the 2p inner-shell region imply a change in the atomic configuration of Ga. This may indeed be the reason for the effect of acetone on the crystallinity of Ga in the crystal growth. Second and more importantly, the Ga sample processed by β-CD (Ga−3a) has higher binding energies of Ga 3d, Ga $2p_{3/2}$, and Ga $2p_{1/2}$ (Table 1 and light-gray arrows in Figure 4) compared to the Ga−1b. Meanwhile, the binding energies of both C 1s and O 1s of β-CD decrease.

This significant finding, concerning the decrease in electron density of inner-shell region of Ga atoms and the increase in electron density of inner-shell region of carbon and oxygen atoms of β-CD, is a direct demonstration that there is an

dx.doi.org/10.1021/ic200137f |Inorg. Chem. 2011, 50, 7988–7996

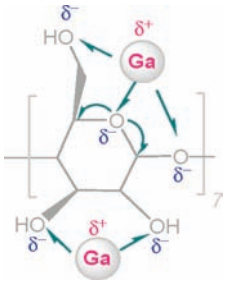

Figure 5. Proposed atom−molecule interaction between Ga and β-CD.

atom−molecule interaction between Ga and β-CD by the electronic shift from Ga atoms to oxygen atoms in the frame structure of β-CD. A schematic diagram illustrating such a possible interaction mechanism is proposed in Figure 5.

The transfer of electron density from Ga atoms to electronegative oxygen atoms leads to a deformation of electron clouds of the carbon atoms linked to the oxygen atoms. This explains the increase of binding energies of 3d, $2p_{3/2}$, and $2p_{1/2}$ of Ga and the decrease of binding energies of C 1s and O 1s of β-CD. Additionally, as seen in Figure 4, the decrease in peak areas of Ga 3d, Ga $2p_{3/2}$, and their satellites is a reflection of decrease in Ga content of the samples.[27]

Thermal Behavior of β-CD and Phase Transition of Ga. The difference in stacking forms, surface structures, and electronic properties of the Ga samples allows us to make a new prediction that both the thermal behavior of β-CD and the phase transition of Ga are expected to be influenced by the atom−molecule interaction between them.

Actually, TG analysis suggests that the reaction 10:1 Ga:β-CD ratio is in effect to be present in the Ga−3a sample and demonstrates that the presence of Ga leads to an earlier degradation of β-CD, with a difference of about 27.5 K between the maximum degradation points of β-CD with and without Ga.[24] Moreover, no further mass loss is observed at higher temperatures (>700 K) in the Ga−3a, but the residual mass (RM, %) of free β-CD always decreases with the increase of temperature. As metallic Ga does not lose mass in the TG temperature range, thermal degradation degree (α, %) of β-CD in pure phase, and the mixed phase can be calculated based on eqs 1 and 2, respectively.

$$\alpha = 1 - \mathrm{RM} \times (1 - r_1)^{-1} \quad (1)$$

$$\alpha = 1 - (\mathrm{RM} - r_2) \times (1 - r_1 - r_2)^{-1} \quad (2)$$

In these equations, r_1 and r_2 express the initial mass fractions of water and Ga in the samples, which were determined by TG analysis and elemental analysis. The water mentioned is related to a small quantity of crystal water originated from CD molecules. TG curve shows the release of the water molecules below 400 K.[24] We note that the α values of free β-CD are always much lower than those of the Ga−3a upon degradation. For example, the α values of free β-CD and the Ga−3a at 620 K are 68.25 and 91.36%, respectively. This result implies that the presence of metallic Ga leads to a more complete degradation of β-CD at the same conditions.

The lower decomposition temperature and the higher degradation degree may be explained by two possible mechanisms. 1) The interaction between β-CD and Ga atoms results in the destruction of hydrogen bonding interactions between β-CD molecules and the weakening of C−O bonds (Figure 5). 2) The high thermal conductivity (40.6 $W \cdot m^{-1} \cdot K^{-1}$) of metallic Ga provides effective heat transport.

Table 2. Enthalpy ($J \cdot g^{-1}$) of Endothermic Phase Transitions of Ga−0, Ga−1b, and Ga−3 Series Samples in the Second and Third Cycles

		Ga phases			
samples	ζ	γ	ε	β	α
Ga−0 (Cycle 2)					109.5
Ga−0 (Cycle 3)					109.5
Ga−1b (Cycle 2)		2.14		3.17	69.58
Ga−1b (Cycle 3)		2.52		2.85	70.82
Ga−3a (Cycle 2)		0.83	1.15	19.04	3.98
Ga−3a (Cycle 3)		0.86	1.18	20.17	1.31
Ga−3b (Cycle 2)	1.10	2.10		4.45	73.88
Ga−3c (Cycle 2)		0.32		1.64	51.95
Ga−3d (Cycle 2)		0.09		0.50	67.86
Ga−3e (Cycle 2)		0.12		0.31	66.44

Sintering experiments in nitrogen atmosphere were conducted to investigate the difference in residual products of β-CD and its mixture with metallic Ga. On the one hand, the two Raman spectra have very similar profiles: two overlapping bands due to the first-order D band at 1368 cm^{-1} and the first-order G band at 1599 cm^{-1},[24,28] and the second-order D band at approximately 2850 cm^{-1}.[29,30] The intensity ratios of D and G bands in the two samples are both 0.83. No signals of metallic Ga are observed. These results reveal the generation of amorphous graphite carbon particles.[31,32]

On the other hand, the XRD patterns confirm the formation of graphite carbon layers through a broad diffraction peak at around 21.9°.[33] Further, a moderate peak at 35.6°, corresponding to the 111 plane of Ga_2O_3 films (JCPDS # 87−1901),[34,35] occurs in the residual product of the Ga−3f. The higher binding energies of core levels in Ga−3f in the XPS analysis provide a support that metallic Ga was oxidized under the above conditions.[24,26] Undoubtedly, some degradation products[36,37] of β-CD are involved in and responsible for the oxidation process.

The melting point of metallic Ga at 302.0 K allows us to examine its state of aggregation by DSC experiments by determining the phase transition of Ga in the samples.

DSC analysis was performed in the temperature range of 203.2 to 333.2 K, and each sample was treated with three continuous cycles using the same specimen. In order to eliminate the effect of thermal history,[38] the second and third cycles are used to discuss the phase and structural changes of the Ga samples. The data reflecting the heat effects corresponding to these changes in seven Ga samples (Ga−0, Ga−1b, and Ga−3 series samples) in the two cycles are listed in Table 2.

The high sensitivity DSC analysis indicates that a series of endothermic transition peaks occur in the Ga samples. For example, there are one, three, and four endothermic peaks in the Ga−0, Ga−1b, and Ga−3a, respectively. The endothermic peaks occurring at about 239, 246, and 258 K correspond to the transformation of three low-temperature metastable phases: γ-, ε-, and β-Ga, respectively.[39−42] The endothermic peak at about 302 K corresponds to the stable α phase of metallic Ga.[42] For the same Ga sample, there is some difference in the values of

dx.doi.org/10.1021/ic200137f |Inorg. Chem. 2011, 50, 7988–7996

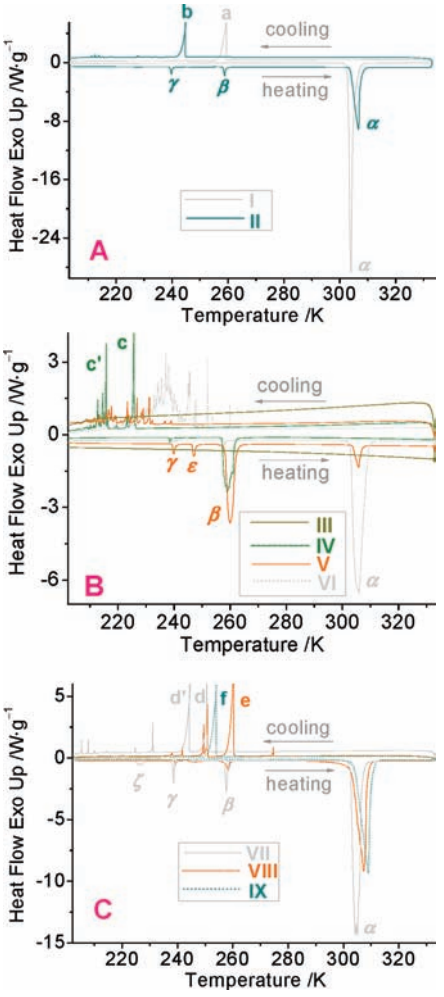

Figure 6. Continuous DSC heating and cooling curves of three group samples in the second cycle. Group A: (I) Ga−0 and (II) Ga−1b. Group B: (III) β-CD, (IV) Ga−2, (V) Ga−3a and (VI) Ga−4, and Group C: (VII) Ga−3b, (VIII) Ga−3c and (IX) Ga−3d.

endothermic enthalpy (Table 2) between the two cycles, but no changes in the number of endothermic transitions were detected. As can be seen by comparison of the data in Table 2, accompanying the increase in the number of metastable phases from Ga−0, Ga−1b to Ga−3a is the large decrease in enthalpy of endothermic phase transition of the stable α phase.

Figure 6 presents the DSC profiles obtained in the second cycle for the eight Ga samples (Ga−0, Ga−1b, Ga−2, Ga−3 series and Ga−4). For pure β-CD, no endothermic and exothermic processes take place in the whole temperature range measured (curve III in part B of Figure 6). Apparently, the number, position and intensity of the endothermic and exothermic peaks observed strongly depend on the structure of the Ga samples. Analyses of variance reveal several significant findings regarding phase transitions of these types of Ga samples.

First, only one signal (very strong) at 303.6 K was seen at curve I in part A of Figure 6 corresponding to α phase in Ga−0. In contrast, three endothermic signals due to γ- (239.7 K), β- (258.8 K), and α-Ga (306.9 K) were detected in the case of Ga−1b (curve II). Moreover, the exothermic processes of the two types of Ga samples, which were assigned to formation of α-Ga crystals in the cooling process, occurred in quite different positions: Ga−0 at 259.3 K (peak a) and Ga−1b at 244.6 K (peak b). The significant difference in peak areas and formation temperatures of α phase between the two Ga samples is attributable to a structural difference between them as described in Figure 1.

Second, and more importantly, the Ga−2 obtained in the presence of α-CD shows only the γ and β metastable phases at 238.5 (very weak signal) and 259.0 K (moderate signal) respectively and does not show any sign of the formation of the thermally stable α phase. The reason may be that the initial eutectic undercooling is so large (two very strong peaks c and c′ occur below 226 K on subsequent cooling) that metastable phases may form instead of a stable α phase.[42] The result is astounding because such a phenomenon is not observed in the cases of the other four Ga samples. This finding is significant and opens up new applications for controlling and configuring various types of Ga phases in physical and chemical systems.

Third, the two Ga samples (Ga−3a and Ga−3b) obtained in the presence of different amount of β-CD present completely different DSC profiles. On the one hand, Ga−3b shows a novel endothermic peak at 226.3 K during heating, suggesting the appearance of a new ζ-Ga phase (curve VII in part C of Figure 6). At the same time, two strong exothermic peaks (d and d′) occur during cooling. On the other hand, Ga−3a shows the existence of ε-Ga phase at 247.1 K instead of ζ-Ga phase, and the endothermic enthalpy corresponding to α phase of the sample is much lower than that of Ga−3b. Effects of Ga/β-CD ratios were further studied using the Ga−3 series samples. Data in Table 2 indicate that there are still observable effects on endothermic enthalpy changes of phase transitions even in the presence of a very low amount of β-CD, and that, the lower the amount of β-CD, the fewer the exothermic signals of phase transitions in the cooling process. Also, it is noted that the metastable phases: ζ-Ga and ε-Ga appearing in Ga−3a and Ga−3b are not observable in the three samples with low percentage of β-CD. The result means that the phase transition of metallic Ga can be modulated by the amount of a variant β-CD.

Fourth, and most importantly, what is surprising is that the DSC cooling traces of the three Ga samples (Ga−2, Ga−3a, Ga−3b, and especially Ga−4), which contain a host component, remain quite rough in the cooling process, leaving numerous exothermic signals. The presence of these signals is certainly associated with the evolution of Ga structures at lower temperatures. It can be explained by the shielding effect of host cavities. Ga atoms entered and deposited onto the sidewalls of the cavities in the cooling process resulting in a broad range of undercooling.

In conclusion, doping various types of CDs into metallic Ga causes different structures of Ga crystals, which is a result of different interactions between Ga and CDs. The regulation in Ga structures is responsible for the existence of multiphases of Ga in the binary systems.

Magnetic Property of Ga Samples. SQUID measurements were made to further explore whether such atom−molecule interactions have the capacity to regulate the magnetic property of metallic Ga.

Two samples, Ga−0 and Ga−3a, were cooled from room temperature to 2.0 K. Then the magnetization (M) was measured both in zero-field-cooled (ZFC) and in field-cooled (FC) states, and data was collected with a 0.2 K step size in an applied field H = 500 Oe. The temperature dependence of the FC and ZFC magnetization is illustrated in Figure 7.

Part A of Figure 7 shows fluctuations in the FC magnetization throughout evolution, as well as in the ZFC magnetization in the range from 5 to 10 K, for the Ga−0 sample. The critical

dx.doi.org/10.1021/ic200137f |Inorg. Chem. 2011, 50, 7988–7996

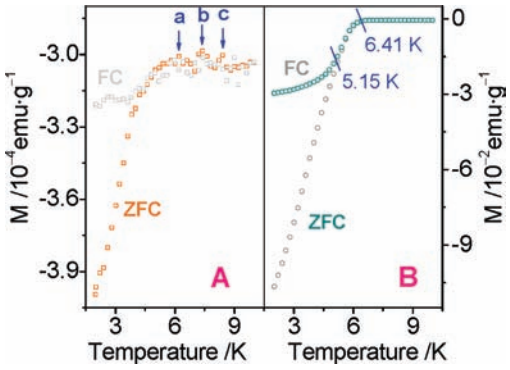

Figure 7. FC and ZFC magnetization curves of Ga−0 (A) and Ga−3a (B) at 500 Oe.

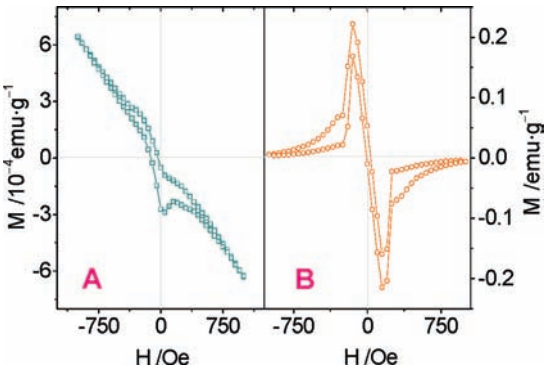

Figure 8. Plots of M vs H of Ga−0 (A) and Ga−3a (B) at 4.5 K.

temperatures (T_c) at 6.2 (arrow a), 7.4 (arrow b), and 8.4 K (arrow c) in the ZFC magnetization curve correspond to the superconducting transition temperatures of β, γ, and amorphous phases of Ga.[43,44] This suggests complex aspects of phase transition properties of free Ga in the temperature scale, which is caused by the effect of a lattice periodic crystal field on the $4p^1$ electron.[45] However, no fluctuations are observed in the FC and ZFC magnetization curves of the Ga−3a sample. Besides, it has a much larger magnetization than Ga−0 at the same temperatures, indicating a decrease in electron density of valence shell of Ga atoms in this case,[46] which is in accordance with XPS analysis. These comparisons demonstrate clearly that the presence of β-CD induces a significant change in the magnetic property of metallic Ga.

Further, as seen in part B of Figure 7, the ZFC curve is temperature independent in the range of 6.5 to 10 K suggesting that the Ga sample is a Pauli paramagnet before the onset of superconductivity. Subsequently, a sharp drop occurs at 6.41 K (T_c), implying the magnetic onset of superconductivity, corresponding to the superconducting phase transition of β-Ga.[43] This phenomenon also appears in the FC curve. After experiencing a rapid increase of M values up to around 5.15 K, the curves split significantly. The ZFC magnetization curve decreases sharply, whereas the FC magnetization curve indicates a plateau.

Typical magnetic hysteresis curves obtained at 4.5 K with a 50 Oe step size for Ga−0 and Ga−3a are depicted in Figure 8 providing further evidence for the superconductivity occurrence. Also, we notice that there is a substantial difference in the dependence of M values on H between them. As can be seen from part A of Figure 8, the magnetization signal of the Ga−0 sample has a full loop but is asymmetric around the zero of the field. And the absolute M value reaches the saturation magnetization (M_s, 6.3×10^{-4} emu·g^{-1}) at 997 Oe. However, the Ga−3a sample not only has a higher M value (6.2×10^{-3} emu·g^{-1}) at this H but also gives an almost symmetric hysteresis loop with the maximum magnetization (M_m) of 0.22 emu·g^{-1} at 147 Oe. The most interesting observation is that the ratio of the maximum of Ga−3a to the maximum of Ga−0 is about 349.

Table 3. Magnetic Parameters of the Ga Samples

	Magnetization (emu·g^{-1})		
samples	M_m	M_s	M_r
Ga−0		6.3×10^{-4}	5.4×10^{-5}
Ga−1a	4.8×10^{-4}	1.6×10^{-4}	8.2×10^{-5}
Ga−1b	1.1×10^{-2}	1.1×10^{-3}	2.9×10^{-4}
Ga−1c	1.0×10^{-3}	6.1×10^{-4}	2.3×10^{-4}
Ga−1d	8.2×10^{-3}	1.1×10^{-3}	7.3×10^{-4}
Ga−2	2.5×10^{-3}	5.2×10^{-4}	1.8×10^{-4}
Ga−3a	2.2×10^{-1}	6.2×10^{-3}	1.2×10^{-2}
Ga−3b	5.8×10^{-1}	3.9×10^{-2}	4.8×10^{-2}
Ga−4	6.6×10^{-2}	4.4×10^{-3}	1.2×10^{-3}

Although there is a large difference in the hysteresis loops of the two Ga samples, both of them indicate a similar shape of conventional type-II superconductors or ceramic high-temperature superconductors, each having a different value of critical magnetic field (H_c).[47] For example, as seen in part A of Figure 8, the superconducting property of the Ga−0 sample can be maintained beyond the magnetic field frame of the study, representing the Meissner effect, that is massive superconductivity. Nevertheless, the Ga−3a sample exhibits the great disadvantage of losing a large amount of its superconductive character even at higher than 147 Oe (H_c).[48] It is proposed that this phenomenon is a reflection of the phase transitions by the introduction of β-CD. In a word, the change in physical property of metallic Ga induced by the presence of β-CD is surprising given the importance of atom−molecule interaction.

Magnetic properties of other Ga samples were also measured in the same manner and magnetic parameters were summarized in Table 3, from which we find that there are significant differences in M_m, M_s, and remanence magnetization (M_r) of Ga−0, Ga−1 series, and Ga/CD samples.

On the one hand, the Ga−1 series samples exhibit completely different magnetic parameters, most of which are larger than those of Ga−0. This provides direct evidence of the distinct influences of various solvents. On the other hand, most Ga/CD samples give much larger magnetic parameters than the Ga−1 series samples reflecting the important role of CD molecules in mediating the magnetic property of metallic Ga.

CONCLUSIONS

This study reveals two striking findings. 1) There are effects of organic solvent media on magnetic property and microstructure of metallic Ga, including surface morphology, stacking behavior and electronic structure, and the extent of effects depends on the polarity of the solvents used. 2) The introduction of a small amount of CDs leads to further change in microstructure, which not only allows the existence of a series of metastable phases of Ga in different forms but also causes the improvement of the magnetic property of Ga.

dx.doi.org/10.1021/ic200137f |*Inorg. Chem.* 2011, 50, 7988–7996

These significant differences between free Ga and the Ga samples crystallized in the presence of the solvent media especially CDs demonstrate the extraordinary effect of atom−molecule interaction in modifying structure, phase transition, and magnetic property of metallic Ga. Although the number of solvents and CDs employed in this work is small, we believe that the findings of our study could reflect a pervasive phenomenon and should be applicable to many branches of natural sciences, including inorganic chemistry, chemical physics, and crystal growth.

■ ASSOCIATED CONTENT

Supporting Information. 1) Photographs of Ga−0 and Ga−1 series samples, 2) TG/DTG curves of β-CD and Ga−3a, 3) Raman spectra of β-CD and Ga−3f after sintering, 4) XRD patterns of β-CD and Ga−3f after sintering, 5) binding energies of some core levels in Ga−3f, and 6) continuous DSC curves of Ga−3e. This material is available free of charge via the Internet at http://pubs.acs.org.

■ AUTHOR INFORMATION

Corresponding Author
*E-mail: solexin@ustc.edu.cn.

■ ACKNOWLEDGMENT

This project was supported by NSFC (No. 21071139).

■ REFERENCES

(1) Wu, P. C.; Khoury, C. G.; Kim, T. H.; Yang, Y.; Losurdo, M.; Bianco, G. V.; Vo-Dinh, T.; Brown, A. S.; Everitt, H. O. *J. Am. Chem. Soc.* **2009**, *131*, 12032–12033.

(2) (a) Sanchez-Sobrado, O.; Thomas, K.; Povey, I.; Pemble, M. E.; Miguez, H. *Small* **2010**, *6*, 1283–1287. (b) Himmel, H. N.; Gaertner, B. *Chem.—Eur. J.* **2004**, *10*, 5936–5941.

(3) (a) Gasparotto, L. H. S.; Borisenko, N.; Hofft, O.; Al-Salman, R.; Maus-Friedrichs, W.; Bocchi, N.; El Abedin, S. Z.; Endres, F. *Electrochim. Acta* **2009**, *55*, 218–226. (b) Baker, R. J.; Jones, C. *Coord. Chem. Rev.* **2005**, *249*, 1857–1869. (c) Wehmschulte, R. J. *Angew. Chem., Int. Ed.* **2010**, *49*, 4708–4709.

(4) (a) Grunenberg, J.; Goldberg, N. *J. Am. Chem. Soc.* **2000**, *122*, 6045–6047. (b) Xie, J. M.; Grev, R. S.; Gu, J. D.; Schaefer, H. F.; Schleyer, P. V.; Su, J. R.; Li, X. W.; Robinson, G. H. *J. Am. Chem. Soc.* **1998**, *120*, 3773–3780.

(5) Chen, X. M.; Fei, G. T.; Zheng, K. *J. Phys. Condens. Mat.* **2009**, *21*, 245403–5.

(6) Gong, X. G.; Chiarotti, G. L.; Parrinello, M.; Tosatti, E. *Phys. Rev. B* **1991**, *43*, 14277–14280.

(7) (a) Evans, M. J.; Holland, G. P.; Garcia-Garcia, F. J.; Haussermann, U. *J. Am. Chem. Soc.* **2008**, *130*, 12139–12147. (b) Chakrapani, V.; Pendyala, C.; Kash, K.; Anderson, A. B.; Sunkara, M. K.; Angus, J. C. *J. Am. Chem. Soc.* **2008**, *130*, 12944–12952.

(8) Fricke, R.; Kosslick, H.; Lischke, G.; Richter, M. *Chem. Rev.* **2000**, *100*, 2303–2405.

(9) (a) Xu, C. X.; Sun, X. W.; Chen, B. J. *Appl. Phys. Lett.* **2004**, *84*, 1540–1542. (b) Rakhshani, A. E.; Bumajdad, A.; Kokaj, J.; Thomas, S. *Appl. Phys. A, Mater.* **2009**, *97*, 759–764.

(10) Bundesmann, C.; Ashkenov, N.; Schubert, M.; Spemann, D.; Butz, T.; Kaidashev, E. M.; Lorenz, M.; Grundmann, M. *Appl. Phys. Lett.* **2003**, *83*, 1974–1976.

(11) Harada, A.; Osaki, M.; Takashima, Y.; Yamaguchi, H. *Acc. Chem. Res.* **2008**, *41*, 1143–1152.

(12) (a) Legrand, F. X.; Hapiot, F.; Tilloy, S.; Guerriero, A.; Peruzzini, M.; Gonsalvi, L.; Monflier, E. *Appl. Catal. A, Gen.* **2009**, *362*, 62–66. (b) Denicourt-Nowicki, A.; Roucoux, A.; Wyrwalski, F.; Kania, N.; Monflier, E.; Ponchel, A. *Chem.—Eur. J.* **2008**, *14*, 8090–8093. (c) Song, L. X.; Wang, H. M.; Xu, P.; Zhang, Z. Q.; Liu, Q. Q. *Bull. Chem. Soc. Jpn.* **2007**, *80*, 2313–2322.

(13) (a) Yamauchi, K.; Miyawaki, A.; Takashima, Y.; Yamaguchi, H.; Harada, A. *Org. Lett.* **2010**, *12*, 1284–1286. (b) Taura, D.; Li, S. J.; Hashidzume, A.; Harada, A. *Macromolecules* **2010**, *43*, 1706–1713. (c) Rungta, P.; Bandera, Y. P.; Tsyalkovsky, V.; Foulger, S. H. *Soft Matter* **2010**, *6*, 6083–6095.

(14) (a) Braga, S. S.; Gago, S.; Seixas, J. D.; Valente, A. A.; Pillinger, M.; Santos, T. M.; Goncalves, I. S.; Romao, C. C. *Inorg. Chim. Acta* **2006**, *359*, 4757–4764. (b) Song, L. X.; Wang, H. M.; Yang, Y.; Xu, P. *Bull. Chem. Soc. Jpn.* **2007**, *80*, 2185–2195. (c) Hubert, C.; Denicourt-Nowicki, A.; Roucoux, A.; Landy, D.; Leger, B.; Crowyn, G.; Monflier, E. *Chem. Commun.* **2009**, 1228–1230. (d) Machut, C.; Mouri-Belabdelli, F.; Cavrot, J. P.; Sayede, A.; Monflier, E. *Green Chem.* **2010**, *12*, 772–775.

(15) (a) Song, L. X.; Xu, P. *J. Phys. Chem. A* **2008**, *112*, 11341–11348. (b) Zhu, L. H.; Song, L. X.; Guo, X. Q.; Dang, Z. *Thermochim. Acta* **2010**, *507−508*, 77–83.

(16) (a) Harata, K. *Chem. Rev.* **1998**, *98*, 1803–1827. (b) Song, L. X.; Yang, J.; Bai, L.; Du, F. Y.; Chen, J.; Wang, M. *Inorg. Chem.* **2011**, *50*, 1682–1688.

(17) (a) Braga, S. S.; Paz, F. A. A.; Pillinger, M.; Seixas, J. D.; Romao, C. C.; Goncalves, I. S. *Eur. J. Inorg. Chem.* **2006**, 1662–1669. (b) Song, L. X.; Wang, H. M.; Guo, X. Q.; Bai, L. *J. Org. Chem.* **2008**, *73*, 8305–8316. (c) Braga, S. S.; Paz, F. A. A.; Mokal, V.; Pillinger, M.; Marques, M. P. M.; Romao, C. C.; Goncalves, I. S. *Drug Future* **2007**, *32*, 101–101.

(18) (a) Song, L. X.; Bai, L. *J. Phys. Chem. B* **2009**, *113*, 11724–11731. (b) Song, L. X.; Du, F. Y.; Guo, X. Q.; Pan, S. Z. *J. Phys. Chem. B* **2010**, *114*, 1738–1744.

(19) (a) Santos, L.; Ghilane, J.; Martin, P.; Lacaze, P. C.; Randriamahazaka, H.; Lacroix, J. C. *J. Am. Chem. Soc.* **2010**, *132*, 1690–1698. (b) Wang, H. M.; Song, L. X. *Chem. Lett.* **2007**, *36*, 596–597.

(20) (a) Ghosn, M. W.; Wolf, C. *J. Am. Chem. Soc.* **2009**, *131*, 16360–16361. (b) Song, L. X.; Wang, M.; Dang, Z.; Du, F. Y. *J. Phys. Chem. B* **2010**, *114*, 3404–3410.

(21) Song, L. X.; Bai, L.; Xu, X. M.; He, J.; Pan, S. Z. *Coord. Chem. Rev.* **2009**, *253*, 1276–1284.

(22) (a) Chachisvilis, M.; Garcia-Ochoa, I.; Douhal, A.; Zewail, A. H. *Chem. Phys. Lett.* **1998**, *293*, 153–159. (b) Zhou, Y.; Yu, S. H.; Thomas, A.; Han, B. H. *Chem. Commun.* **2003**, 262–263. (c) Stith, A.; Hitchens, T. K.; Hinton, D. P.; Berr, S. S.; Driehuys, B.; Brookeman, J. R.; Bryant, R. G. *J. Magn. Reson.* **1999**, *139*, 225–231.

(23) Liu, Z. W.; Bando, Y.; Mitome, M.; Zhan, J. H. *Phys. Rev. Lett.* **2004**, *93*, 095504–4.

(24) See the Supporting Information.

(25) (a) Windisch, C. F.; Henager, C. H.; Engelhard, M. H.; Bennett, W. D. *J. Nucl. Mater.* **2009**, *395*, 23–29. (b) Kundu, S.; Xia, W.; Busser, W.; Becker, M.; Schmidt, D. A.; Havenith, M.; Muhler, M. *Phys. Chem. Chem. Phys.* **2010**, *12*, 4351–4359.

(26) Wagner, C. D.; Riggs, W. M.; Davis, L. E.; Moulder, J. F. *Handbook of X-ray Photoelectron Spectroscopy*; Perkin-Elmer Corporation: Eden Prarie, MN, 1979.

(27) Atuchin, V. V.; Isaenko, L. I.; Kesler, V. G.; Lobanov, S. I. *J. Alloys Compd.* **2010**, *497*, 244–248.

(28) Klinke, C.; Kurt, R.; Bonard, J. M.; Kern, K. *J. Phys. Chem. B* **2002**, *106*, 11191–11195.

(29) Dillon, R. O.; Woollam, J. A.; Katkanant, V. *Phys. Rev. B* **1984**, *29*, 3482–3489.

(30) Wakeland, S.; Martinez, R.; Grey, J. K.; Luhrs, C. C. *Carbon* **2010**, *48*, 3463–3470.

(31) Nistor, L.; Ralchenko, V.; Vlasov, I.; Khomich, A.; Khmelnitskii, R.; Potapov, P.; van Landuyt, J. *Phys. Status Solidi. A* **2001**, *186*, 207–214.

(32) de Clippel, F.; Harkiolakis, A.; Ke, X.; Vosch, T.; Van Tendeloo, G.; Baron, G. V.; Jacobs, P. A.; Denayer, J. F. M.; Sels, B. F. *Chem. Commun.* **2010**, *46*, 928–930.

(33) Saenger, K. L.; Tsang, J. C.; Bol, A. A.; Chu, J. O.; Grill, A.; Lavoie, C. *Appl. Phys. Lett.* **2010**, *96*, 153105–3.

(34) Tian, D. H.; Xue, C. S.; Zhuang, H. Z.; Zhang, X. K.; Wu, Y. X.; He, J. T.; Liu, Y.; Wang, F. X. *J. Cryst. Growth* **2006**, *292*, 298–301.
(35) Ahman, J.; Svensson, G.; Albertsson, J. *Acta Crystallogr., C* **1996**, *52*, 1336–1338.
(36) Song, L. X.; Bai, L. *J. Phys. Chem. B* **2009**, *113*, 9035–9040.
(37) Song, L. X.; Dang, Z. *J. Phys. Chem. B* **2009**, *113*, 4998–5000.
(38) Honcova, P.; Svoboda, R.; Malek, J. *Thermochim. Acta* **2010**, *507*−*508*, 71–76.
(39) (a) He, H.; Fei, G. T.; Cui, P.; Zheng, K.; Liang, L. M.; Li, Y.; De Zhang, L. *Phys. Rev. B* **2005**, *72*, 073310–4. (b) Chen, X. M.; Fei, G. T.; Li, X. F.; Zheng, K.; Zhang, L. D. *J. Phys. Chem. Solids* **2010**, *71*, 918–921.
(40) Di Cicco, A. *Phys. Rev. Lett.* **1998**, *81*, 2942–2945.
(41) Zhang, W. P.; Ratcliffe, C. I.; Moudrakovski, I. L.; Tse, J. S.; Mou, C. Y.; Ripmeester, J. A. *Micropor. Mesopor. Mater.* **2005**, *79*, 195–203.
(42) Bosio, L.; Windsor, C. G. *Phys. Rev. Lett.* **1975**, *35*, 1652–1655.
(43) Teske, D.; Drumheller, J. E. *J. Phys. Condens. Mater.* **1999**, *11*, 4935–4940.
(44) Charnaya, E. V.; Tien, C.; Lee, M. K.; Kumzerov, Y. A. *J. Phys. Condens. Mater.* **2009**, *21*, 455304–6.
(45) Yu, X. Z.; Onose, Y.; Kanazawa, N.; Park, J. H.; Han, J. H.; Matsui, Y.; Nagaosa, N.; Tokura, Y. *Nature* **2010**, *465*, 901–904.
(46) (a) Herng, T. S.; Lau, S. P.; Yu, S. F.; Tsang, S. H.; Teng, K. S.; Chen, J. S. *J. Appl. Phys.* **2008**, *104*, 103104–5. (b) Bonanni, A.; Kiecana, M.; Simbrunner, C.; Li, T.; Sawicki, M.; Wegscheider, M.; Quast, M.; Przybylinska, H.; Navarro-Quezada, A.; Jakiela, R.; Wolos, A.; Jantsch, W.; Dietl, T. *Phys. Rev. B* **2007**, *75*, 125210–18.
(47) (a) Charnaya, E. V.; Tien, C.; Wur, C. S.; Kumzerov, Y. A. *Physica C* **1996**, *269*, 313–324. (b) Charnaya, E. V.; Kumzerov, Y. A.; Tien, C.; Wur, C. S. *Solid State Commun.* **1995**, *94*, 635–641. (c) Nabialek, A.; Szymczak, H.; Piotrowski, K.; Chabanenko, V.; Pakiela, Z. *Physica C* **1999**, *321*, 49–58.
(48) (a) Dersch, H.; Blatter., G. *Phys. Rev. B* **1988**, *38*, 11391–11404. (b) Bean, C. P. *Phys. Rev. Lett.* **1962**, *8*, 250–253.